

Building Continuous Time Crystals from Rare Events

R. Hurtado-Gutiérrez^{1,2,*}, F. Carollo^{3,†}, C. Pérez-Espigares^{1,2,‡,¶} and P. I. Hurtado^{1,2,§,¶}

¹*Departamento de Electromagnetismo y Física de la Materia, Universidad de Granada, Granada 18071, Spain*

²*Instituto Carlos I for Theoretical and Computational Physics, Universidad de Granada, Granada 18071, Spain*

³*Institut für Theoretische Physik, Universität Tübingen, Auf der Morgenstelle 14, 72076 Tübingen, Germany*

 (Received 13 December 2019; accepted 17 September 2020; published 14 October 2020)

Symmetry-breaking dynamical phase transitions (DPTs) abound in the fluctuations of non-equilibrium systems. Here, we show that the spectral features of a particular class of DPTs exhibit the fingerprints of the recently discovered time-crystal phase of matter. Using Doob's transform as a tool, we provide a mechanism to build classical time-crystal generators from the rare event statistics of some driven diffusive systems. An analysis of the Doob's smart field in terms of the order parameter of the transition then leads to the time-crystal lattice gas (TCLG), a model of driven fluid subject to an external packing field, which presents a clear-cut steady-state phase transition to a time-crystalline phase characterized by a matter density wave, which breaks continuous time-translation symmetry and displays rigidity and long-range spatiotemporal order, as required for a time crystal. A hydrodynamic analysis of the TCLG transition uncovers striking similarities, but also key differences, with the Kuramoto synchronization transition. Possible experimental realizations of the TCLG in colloidal fluids are also discussed.

DOI: [10.1103/PhysRevLett.125.160601](https://doi.org/10.1103/PhysRevLett.125.160601)

Introduction.—Most symmetries in nature can be spontaneously broken (gauge symmetries, rotational invariance, discrete symmetries, etc.), with the system ground state showing fewer symmetries than the associated action. A good example is the spatial-translation symmetry, which breaks, spontaneously giving rise to new phases of matter characterized by crystalline order, accompanied by a number of distinct physical features such as rigidity, long-range order or Bragg peaks [1]. Time-translation symmetry, on the other hand, seemed to be special and fundamentally unbreakable. This changed when Wilczek and Shapere proposed the concept of time crystals [2,3], i.e., systems whose ground state spontaneously breaks time-translation symmetry and thus exhibits enduring periodic motion. This concept, though natural, has stirred a vivid debate among physicists, leading to some clear-cut conclusions [4–8]. Several no-go theorems have been proven that forbid time-crystalline order in equilibrium systems under rather general conditions [9–11], though time crystals are still possible out of equilibrium. In particular, periodically driven (Floquet) systems have been shown to display spontaneous breaking of discrete time-translation symmetry via subharmonic entrainment [12–16]. These so-called discrete time crystals, recently observed in the lab [16–18], are robust against environmental dissipation [19–24] and have also classical counterparts [25,26]. In any case, the possibility of spontaneous breaking of continuous time-translation symmetry remains puzzling (see, however, [27–30]).

Here, we propose an alternative route to search for time-crystalline order in classical settings, based on the recent observation of spontaneous symmetry breaking in the dynamical fluctuations of many-body systems [31–62]. Such fluctuations or rare events concern time-integrated observables and are highly unlikely to occur, since their probability decays exponentially with time, thus following a large deviation principle [63]. However, when these fluctuations come about, they may lead to dynamical phase transitions (DPTs), which manifest as drastic changes in the trajectories of the system and have been recently found in many contexts [31,34,57,64–67]. In particular, second-order DPTs are associated with the emergence of symmetry-broken structures [32,33,39,41,42,45,51,52,59,68]. This is the case of a paradigmatic classical model of particle transport: the weakly asymmetric simple exclusion process (WASEP) in $1d$ [41,54,65,69–72]. The periodic WASEP is a driven diffusive system that, in order to sustain a time-integrated current fluctuation well below its average, develops a jammed density wave or rotating condensate to hinder particle transport and thus facilitate the fluctuation [32,41]. This is displayed in the insets to Fig. 1(a) [41], where a rotating condensate arises for a subcritical biasing field $\lambda < \lambda_c$, which drives the system well below its average stationary current—corresponding to $\lambda = 0$. This DPT is captured by a packing order parameter r , which measures the accumulation of particles around the center of mass of the system; see Fig. 1(a). Such DPT breaks the continuous time-translational symmetry of the original action, thus

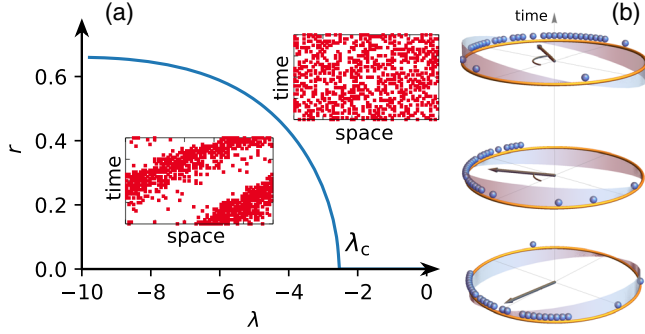


FIG. 1. (a) Packing order parameter $r(\lambda)$ for the DPT in $1d$ WASEP as a function of the biasing field λ . Inset: Spacetime trajectories for current fluctuations above (top) and below (bottom) the critical point. Note the density wave in the latter case. (b) Time-crystal lattice gas with a packing field (shaded curve), which pushes particles lagging behind the center of mass while restraining those moving ahead, a mechanism that leads to a rotating condensate. The arrow locates the condensate center of mass, with a magnitude $\propto r_c$.

opening the door to its use as a resource to build continuous time crystals.

In this Letter, we report three main results. First, we demonstrate that the rotating condensate corresponds to a time-crystal phase at the fluctuating level. We do this by exploring the spectral fingerprints of the DPT present in the WASEP. In particular, we show that the spectrum of the tilted generator describing current fluctuations in this model becomes asymptotically gapless for currents below a critical threshold. Here, a macroscopic fraction of eigenvalues shows a vanishing real part of the gap as the system size $L \rightarrow \infty$, while developing a band structure in the imaginary axis (see Fig. 2), which is the hallmark of time crystals [27]. Interestingly, these rare events can be made typical (i.e., a steady-state property) by virtue of Doob's transform [73–80], which can be interpreted in terms of the original dynamics supplemented with a smart driving field. The second main result consists in showing that this smart field acts as a packing field, pushing particles that lag behind the condensate's center of mass while restraining those moving ahead. This amplifies naturally occurring fluctuations of the packing parameter [see Fig. 1(b)], a nonlinear feedback mechanism (formally reminiscent of the Kuramoto synchronization transition [81–84]), which eventually leads to a time-crystal phase. These observations lead us to the third main result, which distills the key properties of Doob's smart field to introduce the time-crystal lattice gas (TCLG). Numerical simulations and a local stability analysis of its hydrodynamics confirm that the TCLG exhibits a steady-state phase transition to a time-crystalline phase with a matter wave, which breaks continuous time-translation symmetry and displays rigidity, robust coherent periodic motion, and long-range spatiotemporal order despite the stochasticity of the underlying dynamics.

Model.—The WASEP belongs to a broad class of driven diffusive systems of fundamental interest [64,85,86]. Microscopically, it consists of N particles evolving in a $1d$ lattice of $L \geq N$ sites subject to periodic boundary conditions, so the total density is $\rho_0 = N/L$. Each lattice site may be empty or occupied by one particle at most, so a microscopic configuration is given by $C = \{n_k\}_{k=1,\dots,L}$, with $n_k = 0, 1$ the occupation number of the k th site, and $N = \sum_{k=1}^L n_k$. Particles may hop randomly to empty neighboring sites along the $\pm x$ direction with rates $p_{\pm} = \frac{1}{2}e^{\pm E/L}$, with E an external field, which drives the system to a nonequilibrium steady state characterized by an average current $\langle q \rangle = \rho_0(1 - \rho_0)E$ and a homogeneous density profile $\langle n_k \rangle = \rho_0 \forall k$. Configurations can be encoded as vectors in a Hilbert space [87], $|C\rangle = \otimes_{k=1}^L (n_k, 1 - n_k)^T$, with T denoting transposition, and the system information at time t is stored in a vector $|P_t\rangle = [P_t(C_1), P_t(C_2), \dots]^T = \sum_i P_t(C_i)|C_i\rangle$, with $P_t(C_i)$ representing the probability of configuration C_i . This probability vector is normalized, $\langle -|P_t\rangle = 1$, with $\langle -| = \sum_i \langle C_i|$, and $\langle C_i|C_j\rangle = \delta_{ij}$. $|P_t\rangle$ evolves in time according to a master equation $\partial_t |P_t\rangle = \mathbb{W}|P_t\rangle$, where \mathbb{W} defines the Markov generator of the dynamics (see below). At the macroscopic level, driven lattice gases like WASEP are characterized by a density field $\rho(x, t)$ which obeys a hydrodynamic equation [88]

$$\partial_t \rho = -\partial_x [-D(\rho)\partial_x \rho + \sigma(\rho)E], \quad (1)$$

with $D(\rho)$ and $\sigma(\rho)$ the diffusivity and mobility coefficients, which for WASEP are $D(\rho) = 1/2$ and $\sigma(\rho) = \rho(1 - \rho)$.

Fluctuations.—We consider now the statistics of an ensemble of trajectories conditioned to a given space- and time-integrated current Q during a long time t . As in equilibrium statistical physics [63], this trajectory ensemble is fully characterized by a dynamical partition function, $Z_t(\lambda) = \sum_Q P_t(Q)e^{\lambda Q}$, where $P_t(Q)$ is the probability of trajectories of duration t with total current Q , or equivalently by the associated dynamical free energy $\theta(\lambda) = \lim_{t \rightarrow \infty} t^{-1} \ln Z_t(\lambda)$. The variable λ is an intensive biasing field, conjugated to the extensive current Q in a way similar to the relation between temperature and energy in equilibrium systems [76]. Negative (positive) values of λ bias the statistics of Q toward currents lower (larger) than the average stationary value, which corresponds to $\lambda = 0$ [38]. The statistics of the configurations associated with a rare event of parameter λ are captured by a vector $|P_t(\lambda)\rangle$, which evolves in time according to a deformed master equation $\partial_t |P_t(\lambda)\rangle = \mathbb{W}^\lambda |P_t(\lambda)\rangle$, with \mathbb{W}^λ a tilted generator, which biases the original dynamics in order to favor large or low currents according to the sign of λ . It can be shown [63,65,89] that $\theta(\lambda)$ is the largest eigenvalue of \mathbb{W}^λ , as $Z_t(\lambda) = \langle -|P_t(\lambda)\rangle$. For WASEP [36,38],

$$\mathbb{W}^\lambda = \sum_{k=1}^L \left[\frac{1}{2} e^{\frac{\lambda+E}{L}} \hat{\sigma}_{k+1}^+ \hat{\sigma}_k^- + \frac{1}{2} e^{-\frac{\lambda+E}{L}} \hat{\sigma}_k^+ \hat{\sigma}_{k+1}^- - \frac{1}{2} e^{\frac{E}{L}} \hat{n}_k (\mathbb{I} - \hat{n}_{k+1}) - \frac{1}{2} e^{-\frac{E}{L}} \hat{n}_{k+1} (\mathbb{I} - \hat{n}_k) \right], \quad (2)$$

where $\hat{\sigma}_k^\pm$ are creation and annihilation operators acting on site $k \in [1, L]$, \mathbb{I} is the identity matrix, and $\hat{n}_k = \hat{\sigma}_k^+ \hat{\sigma}_k^-$ is the number operator. Note that the original Markov generator is just $\mathbb{W} \equiv \mathbb{W}^{\lambda=0}$, while $\mathbb{W}^{\lambda \neq 0}$ does not conserve probability (i.e., $\langle -|\mathbb{W}^{\lambda \neq 0} \rangle \neq 0$).

Spectral analysis of the DPT.—The WASEP has been shown to exhibit a DPT [32,41,65] to a time-translation symmetry-broken phase for $|E| > E_c \equiv \pi/\sqrt{\rho_0(1-\rho_0)}$ and $\lambda_c^- < \lambda < \lambda_c^+$, with $\lambda_c^\pm = \pm\sqrt{E^2 - E_c^2} - E$, where $\theta(\lambda)$ develops a second-order singularity, and a macroscopic jammed condensate emerges to hinder particle transport and thus aid low current fluctuations; see bottom inset in Fig. 1(a). This DPT is well captured by the packing order parameter $r(\lambda)$, the λ -ensemble average of $r_C \equiv |z_C|$, with $z_C \equiv N^{-1} \sum_{k=1}^N e^{i2\pi x_k(C)/L} = r_C e^{i\phi_C}$, and $x_k(C)$ the lattice position of particle k in configuration C ; see Fig. 1(a). Note that $r_C = |z_C|$ and $\phi_C = \arg(z_C)$ are the well-known Kuramoto order parameters of synchronization [81–84], measuring in this case the particles' spatial coherence and the center-of-mass angular position, respectively, thus capturing the transition from the homogeneous to the density wave phase. The spectrum of \mathbb{W}^λ codifies all the information on this DPT. In particular, let $|R_i^\lambda\rangle$ and $\langle L_i^\lambda|$ be the i th ($i = 0, 1, \dots, 2^L - 1$) right and left eigenvectors of \mathbb{W}^λ , respectively, so $\mathbb{W}^\lambda |R_i^\lambda\rangle = \theta_i(\lambda) |R_i^\lambda\rangle$ and $\langle L_i^\lambda | \mathbb{W}^\lambda = \theta_i(\lambda) \langle L_i^\lambda|$, with $\theta_i(\lambda) \in \mathbb{C}$ the associated eigenvalue ordered according to their real part (largest first) so that $\theta(\lambda) = \theta_0(\lambda)$. Figures 2(a) and 2(b) show the spectrum of \mathbb{W}^λ for $L = 24$, $\rho_0 = 1/3$, $E = 10$, and two values of the biasing field λ , one subcritical [Fig. 2(a)] and another once the DPT has kicked in [Fig. 2(b)]. Clearly, the structure of the spectrum in the complex plane changes radically between the two phases. In particular, while the spectrum is gapped (in the sense that $\text{Re}[\theta_i - \theta_0] < 0$ for $i > 0$) for any $\lambda < \lambda_c^-$ or $\lambda > \lambda_c^+$ [Fig. 2(c)], the condensate phase ($\lambda_c^- < \lambda < \lambda_c^+$) is characterized by a vanishing gap in the real part of a macroscopic fraction of eigenvalues as $L \rightarrow \infty$, which decays as a power-law with $1/L$; see Fig. 2(d). Moreover, the imaginary parts of the gap-closing eigenvalues exhibit a clear band structure with a constant frequency spacing δ , which can be directly linked with the velocity v of the moving condensate, $\delta = 2\pi v/L$ [see dashed horizontal lines in Fig. 2(d)], all standard features of a time-crystal phase [4–8]. Indeed, the emergence of a multiple [$\mathcal{O}(L)$ -fold] degeneracy as L increases for $\lambda_c^- < \lambda < \lambda_c^+$ signals the appearance of different competing (symmetry-broken) states, related to the invariance of the condensate against integer translations along the lattice.

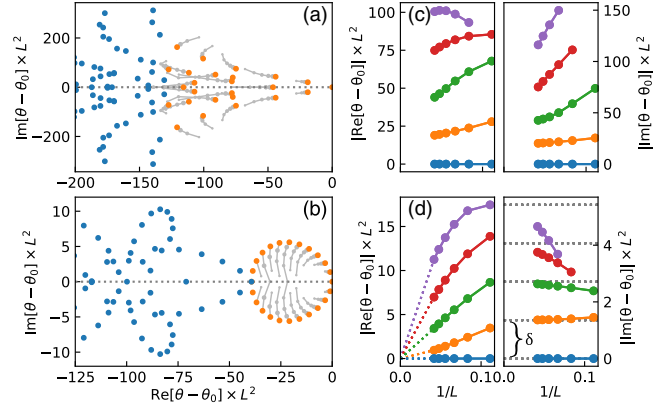


FIG. 2. Diffusively scaled spectrum of the tilted generator \mathbb{W}^λ for $E = 10$. (a) Homogeneous phase for $\lambda = -1$. (b) Condensate phase for $\lambda = -9$. Big colored points correspond to $L = 24$, while small light gray points represent the leading eigenvalues for smaller lattice sizes ($L = 9, 12, 15, 18, 21$), showing their evolution as L increases. (c),(d) Finite-size scaling analysis for the real and imaginary parts of the leading eigenvalues in the homogeneous (c) and condensate (d) phases. The real parts converge to zero as a power law of $1/L$ in the condensate phase, while the imaginary parts exhibit a clear band structure with constant frequency spacing δ , proportional to the condensate velocity.

This DPT at the fluctuating level has therefore the fingerprints of a time-crystal phase, thus enabling a path to engineer these novel phases of matter in driven diffusive systems.

Doob's smart field.—We can now turn the condensate dynamical phase into a true time-crystal phase of matter by making typical the rare events for any λ , i.e., by transforming the nonstochastic generator \mathbb{W}^λ into a physical generator \mathbb{W}_D^λ via the Doob's transform $\mathbb{W}_D^\lambda \equiv \mathbb{L}_0 \mathbb{W}^\lambda \mathbb{L}_0^{-1} - \theta_0(\lambda)$, with \mathbb{L}_0 a diagonal matrix with elements $(\mathbb{L}_0)_{ii} = \langle L_0^\lambda | C_i \rangle$ [73–80]. \mathbb{W}_D^λ is now a probability-conserving stochastic matrix, $\langle -|\mathbb{W}_D^\lambda = 0$, with a spectrum simply related to that of \mathbb{W}^λ , i.e., $\theta_i^D(\lambda) = \theta_i(\lambda) - \theta_0(\lambda)$, with $|R_{i,D}^\lambda\rangle = \mathbb{L}_0 |R_i^\lambda\rangle$, and $\langle L_{i,D}^\lambda| = \langle L_i^\lambda | \mathbb{L}_0^{-1}$, generating in the steady state the same trajectory statistics as \mathbb{W}^λ . To better understand the underlying physics, we now write Doob's dynamics in terms of the original WASEP dynamics supplemented by a smart field E_λ^D ; i.e., we define $(\mathbb{W}_D^\lambda)_{ij} = (\mathbb{W})_{ij} \exp[q_{C_i C_j} (E_\lambda^D)_{ij}/L]$, with $(\mathbb{W}_D^\lambda)_{ij} = \langle C_i | \mathbb{W}_D^\lambda | C_j \rangle$ and $q_{C_i C_j} = \pm 1$ the direction of the particle jump in the transition $C_j \rightarrow C_i$. Together with the definition of \mathbb{W}_D^λ , this leads to

$$(E_\lambda^D)_{ij} = \lambda + q_{C_i C_j} L \ln \left(\frac{\langle L_0^\lambda | C_i \rangle}{\langle L_0^\lambda | C_j \rangle} \right). \quad (3)$$

E_λ^D can be interpreted as the external field needed to make typical a rare event of bias field λ . In order to disentangle the nonlocal complexity of Doob's smart field, we scrutinize its dependence on the packing parameter r_C .

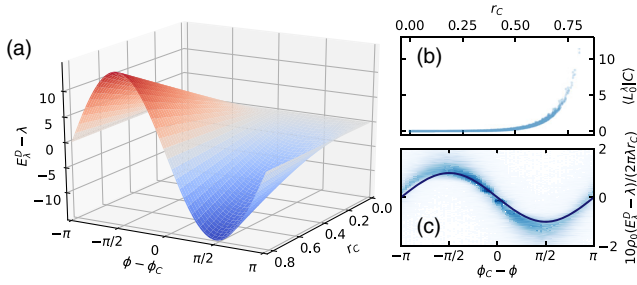


FIG. 3. (a) Smart packing field for $\rho_0 = 1/3$ and $\lambda = -9$ as a function of packing order parameter r_C and the angular distance to the center-of-mass position. (b) $\langle L_0^\lambda | C \rangle$ versus the packing order parameter r_C for $L = 24$, $\rho_0 = 1/3$, $E = 10$, $\lambda = -9$ (condensate phase), and a large sample of microscopic configurations. (c) Angular dependence of the Doob's smart field with respect to the center-of-mass angular location for a large sample of microscopic configurations and the same parameters, together with the $\sin(\phi_k - \phi_C)$ prediction (line).

In particular, Fig. 3(b) plots the projections $\langle L_0^\lambda | C \rangle$ versus the packing parameter r_C for a large sample of microscopic configurations C , as obtained for $L = 24$, $\rho_0 = 1/3$, and $\lambda = -9$ (condensate phase). Interestingly, this shows that $\langle L_0^\lambda | C \rangle \simeq f_{\lambda,L}(r_C)$ to a high degree of accuracy, with $f_{\lambda,L}(r)$ some unknown λ - and L -dependent function of the packing parameter. This means, in particular, that the Doob's smart field $(E_\lambda^D)_{ij}$ depends essentially on the packing parameter of configurations C_i and C_j , a radical simplification. Moreover, as elementary transitions involve just a local particle jump, the resulting change on the packing parameter is perturbatively small for large enough L . In particular, if C'_k is the configuration that results from C after a particle jump at site $k \in [1, L]$, we have that $r_{C'_k} \simeq r_C + 2\pi q_{C'_k C} (\rho_0 L^2)^{-1} \sin(\phi_C - \phi_k)$, with $\phi_k \equiv 2\pi k/L$. The Doob's smart field for this transition is then $(E_\lambda^D)_{C'_k C} \simeq \lambda + 2\pi(\rho_0 L)^{-1} g_{\lambda,L}(r_C) \sin(\phi_C - \phi_k)$, with $g_{\lambda,L}(r) \equiv f_{\lambda,L}(r)/f_{\lambda,L}(r)$, and we empirically find a linear dependence $g_{\lambda,L}(r) \approx -\lambda L r/10$ near the critical point λ_c^+ . This is confirmed in Fig. 3(c), where we plot $10\rho_0[(E_\lambda^D)_{C'_k C} - \lambda]/(2\pi\lambda r_C)$, obtained from Eq. (3) for a large sample of connected configurations $C \rightarrow C'_k$ as a function of $\phi_C - \phi_k$. Similar effective potentials for atypical fluctuations have been found in other driven systems [80,90]. In this way, $(E_\lambda^D - \lambda)$ acts as a packing field on a given configuration C , pushing particles that lag behind the center of mass while restraining those moving ahead [see Fig. 3(a)], with an amplitude proportional to the packing parameter r_C and λ . This nonlinear feedback mechanism, which competes with the diffusive tendency to flatten profiles and the pushing constant field, amplifies naturally occurring fluctuations of the packing parameter, leading eventually to a time-crystal phase for $\lambda_c^- < \lambda < \lambda_c^+$.

Time-crystal lattice gas.—Inspired by the results of the previous analysis, we now simplify the Doob's smart field to introduce the time-crystal lattice gas. This is a

variant of the 1d WASEP, where a particle at site k hops stochastically under a configuration-dependent packing field $E_\lambda(C; k) = E + \lambda + 2\lambda r_C \sin(\phi_k - \phi_C)$, with E being a constant external field and λ now a control parameter. We note that this smart field can be also written as a Kuramoto-like long-range interaction term $E_\lambda(C; k) = E + \lambda + (2\lambda/N) \sum_{j \neq k} \sin(\phi_k - \phi_j)$, highlighting the link between the TCLG and the Kuramoto model of synchronization [81–84]. However, we stress that this link is only formal, as the Kuramoto model lacks any particle transport in real space. According to the discussion above, we expect this lattice gas to display a putative steady-state phase transition to a time-crystal phase with a rotating condensate at some critical λ_c as $L \rightarrow \infty$ (due to the Perron-Frobenius theorem). To test this picture, we performed extensive Monte Carlo simulations and a finite-size scaling analysis of the TCLG at density $\rho_0 = 1/3$. The average packing parameter $\langle r \rangle$ increases steeply but continuously for $\lambda < \lambda_c = -\pi/(1 - \rho_0) \approx -4.7$ [see Fig. 4(a)], converging toward the macroscopic hydrodynamic prediction (see below) as $L \rightarrow \infty$. Moreover, the associated susceptibility, as measured by the packing fluctuations $\langle r^2 \rangle - \langle r \rangle^2$, exhibits a well-defined peak around λ_c , which sharpens as L grows and is compatible with a divergence in the thermodynamic limit [Fig. 4(b)]. The critical point location can be inferred from the crossing of the finite-size Binder cumulants $U_4(L) = 1 - \langle r^4 \rangle / (3\langle r^2 \rangle^2)$ for different L 's [see Fig. 4(c)] and agrees with the hydrodynamic value for λ_c . Interestingly, the average density at a given point exhibits persistent oscillations as a function of time with period v^{-1} (in the diffusive timescale), [see Fig. 4(d)], with v the condensate velocity, a universal feature of time crystals [2–28], and converges toward the hydrodynamic

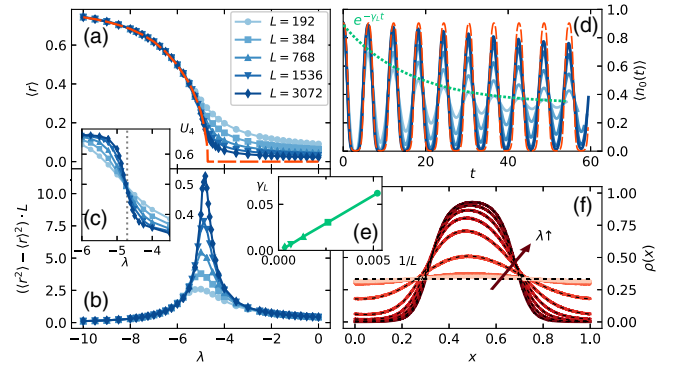


FIG. 4. Numerics for the time-crystal lattice gas. Average packing order parameter (a), its fluctuations (b), and Binder's cumulant (c) measured for $\rho_0 = 1/3$, $E = 10$ and different L . (d) Local density as a function of time and different L 's in the time-crystal phase ($\lambda = -9$). Note the persistent oscillations typical of time crystals. (e) Decay of the oscillations damping rate as $L \rightarrow \infty$, a clear sign of the rigidity of the time-crystal phase in the thermodynamic limit. (f) Average density profile of the condensate for $L = 3072$ and varying λ . Dashed lines correspond to hydrodynamic predictions.

(undamped) periodic prediction as $L \rightarrow \infty$. Indeed, the finite-size damping rate of oscillations, γ_L , obtained from an exponential fit to the envelope of $\langle n_0(t) \rangle$, decays to zero in the thermodynamic limit [Fig. 4(e)], a clear signature of the rigidity of the long-range spatiotemporal order emerging in the time-crystal phase of TCLG. We also measured the average density profile of the moving condensate [see Fig. 4(f)], which becomes highly nonlinear deep into the time-crystal phase. In the macroscopic limit, one can show using a local equilibrium approximation [91–96] that the TCLG is described by a hydrodynamic equation (1) with a ρ -dependent local field $E_\lambda(\rho; x) = E + \lambda + 2\lambda r_\rho \sin(2\pi x - \phi_\rho)$, with $r_\rho = |z_\rho|$, $\phi_\rho = \arg(z_\rho)$, and $z_\rho = \rho_0^{-1} \int_0^1 dx \rho(x) e^{i2\pi x}$ the field-theoretic generalization of our complex order parameter. A local stability analysis then shows [39,54,65] that the homogeneous solution $\rho(x, t) = \rho_0$ becomes unstable at $\lambda_c = -2\pi\rho_0 D(\rho_0)/\sigma(\rho_0) = -\pi/(1 - \rho_0)$, where a ballistic condensate emerges. Hydrodynamic predictions are fully confirmed in simulations; see Fig. 4. Note that the TCLG hydrodynamics is similar to the continuous limit of the Kuramoto model [84], with the peculiarity that for TCLG, the mobility $\sigma(\rho)$ is quadratic in ρ (a reflection of microscopic particle exclusion), while it is linear for Kuramoto.

Conclusion.—We provide here a new mechanism to engineer time-crystalline order in driven diffusive media by making typical rare trajectories that break time-translation symmetry and physically based on the idea of a packing field, which triggers a condensation instability. The modern experimental control of colloidal fluids trapped in quasi-1d periodic structures, such as circular channels [97,98] or optical traps based, e.g., on Bessel rings or optical vortices [99–101], together with feedback-control force protocols to implement the nonlinear packing field $E_\lambda(C; k)$ using optical tweezers [102–107], may allow the engineering and direct observation of this time-crystal phase, opening the door to further experimental advances in this active field. Moreover, the ideas developed in this Letter can be further exploited in $d > 1$, where DPTs exhibit a much richer phenomenology [54,108], with different spatiotemporal symmetry-broken fluctuation phases separated by lines of first- and second-order DPTs, competing density waves and coexistence. This may lead, via the Doob’s transform pathway here described, to materials with a rich phase diagram composed of multiple spacetime-crystalline phases.

The authors thank F. Gambetta and Raúl A. Rica for insightful discussions. The research leading to these results has received funding from the Spanish Ministerio de Economía y Competitividad Project No. FIS2017-84256-P, EPSRC Grant No. EP/N03404X/1, and from the European Regional Development Fund, Junta de Andalucía-Consejería de Economía y Conocimiento, Ref. A-FQM-175-UGR18. R. H. G. thanks funding from the Spanish Ministerio de Ciencia, Innovación y

Universidades fellowship FPU17/02191. C. P. E. acknowledges funding from the European Union’s Horizon 2020 research and innovation programme under the Marie Skłodowska-Curie Cofund Programme Athenea3I Grant Agreement No. 754446. F. C. acknowledges support through a Teach@Tübingen Fellowship. We are also grateful for the computational resources and assistance provided by PROTEUS, the supercomputing center of the Institute Carlos I for Theoretical and Computational Physics at the University of Granada, Spain.

*rhurtado@onsager.ugr.es

†federico.carollo@uni-tuebingen.de

‡carlosperez@ugr.es

§phurtado@onsager.ugr.es

¶These authors contributed equally to this work.

- [1] P. M. Chaikin and T. C. Lubensky, *Principles of Condensed Matter Physics* (Cambridge University Press, Cambridge, 2000), Vol. 1.
- [2] F. Wilczek, Quantum Time Crystals, *Phys. Rev. Lett.* **109**, 160401 (2012).
- [3] A. Shapere and F. Wilczek, Classical Time Crystals, *Phys. Rev. Lett.* **109**, 160402 (2012).
- [4] J. Zakrzewski, Crystals of time, *Physics* **5**, 116 (2012).
- [5] R. Moessner and S. L. Sondhi, Equilibration and order in quantum Floquet matter, *Nat. Phys.* **13**, 424 (2017).
- [6] P. Richerme, How to create a time crystal, *Physics* **10**, 5 (2017).
- [7] N. Y. Yao and C. Nayak, Time crystals in periodically driven systems, *Phys. Today* **71** No. 9, 40 (2018).
- [8] K. Sacha and J. Zakrzewski, Time crystals: A review, *Rep. Prog. Phys.* **81**, 016401 (2018).
- [9] P. Bruno, Impossibility of Spontaneously Rotating Time Crystals: A No-Go Theorem, *Phys. Rev. Lett.* **111**, 070402 (2013).
- [10] P. Nozières, Time crystals: Can diamagnetic currents drive a charge density wave into rotation?, *Europhys. Lett.* **103**, 57008 (2013).
- [11] H. Watanabe and M. Oshikawa, Absence of Quantum Time Crystals, *Phys. Rev. Lett.* **114**, 251603 (2015).
- [12] V. Khemani, A. Lazarides, R. Moessner, and S. L. Sondhi, Phase Structure of Driven Quantum Systems, *Phys. Rev. Lett.* **116**, 250401 (2016).
- [13] C. W. von Keyserlingk, V. Khemani, and S. L. Sondhi, Absolute stability and spatiotemporal long-range order in Floquet systems, *Phys. Rev. B* **94**, 085112 (2016).
- [14] D. V. Else, B. Bauer, and C. Nayak, Floquet Time Crystals, *Phys. Rev. Lett.* **117**, 090402 (2016).
- [15] F. M. Gambetta, F. Carollo, M. Marcuzzi, J. P. Garrahan, and I. Lesanovsky, Discrete Time Crystals in the Absence of Manifest Symmetries or Disorder in Open Quantum Systems, *Phys. Rev. Lett.* **122**, 015701 (2019).
- [16] N. Y. Yao, A. C. Potter, I.-D. Potirniche, and A. Vishwanath, Discrete Time Crystals: Rigidity, Criticality, and Realizations, *Phys. Rev. Lett.* **118**, 030401 (2017).
- [17] J. Zhang, P. W. Hess, A. Kyprianidis, P. Becker, A. Lee, J. Smith, G. Pagano, I.-D. Potirniche, A. C. Potter,

- A. Vishwanath *et al.*, Observation of a discrete time crystal, *Nature (London)* **543**, 217 (2017).
- [18] S. Choi, J. Choi, R. Landig, G. Kucsko, H. Zhou, J. Isoya, F. Jelezko, S. Onoda, H. Sumiya, V. Khemani *et al.*, Observation of discrete time-crystalline order in a disordered dipolar many-body system, *Nature (London)* **543**, 221 (2017).
- [19] K. Nakatsugawa, T. Fujii, and S. Tanda, Quantum time crystal by decoherence: Proposal with an incommensurate charge density wave ring, *Phys. Rev. B* **96**, 094308 (2017).
- [20] A. Lazarides and R. Moessner, Fate of a discrete time crystal in an open system, *Phys. Rev. B* **95**, 195135 (2017).
- [21] Z. Gong, R. Hamazaki, and M. Ueda, Discrete Time-Crystalline Order in Cavity and Circuit QED Systems, *Phys. Rev. Lett.* **120**, 040404 (2018).
- [22] K. Tucker, B. Zhu, R.J. Lewis-Swan, J. Marino, F. Jiménez, J.G. Restrepo, and A.M. Rey, Shattered time: Can a dissipative time crystal survive many-body correlations?, *New J. Phys.* **20**, 123003 (2018).
- [23] J. O'Sullivan, O. Lunt, C. W. Zollitsch, M. L. W. Thewalt, J.J.L. Morton, and A. Pal, Dissipative discrete time crystals, [arXiv:1807.09884](https://arxiv.org/abs/1807.09884).
- [24] A. Lazarides, S. Roy, F. Piazza, and R. Moessner, Time crystallinity in dissipative Floquet systems, *Phys. Rev. Research* **2**, 022002 (2020).
- [25] N. Y. Yao, C. Nayak, L. Balents, and M. P. Zaletel, Classical discrete time crystals, *Nat. Phys.* **16**, 438 (2020).
- [26] F. M. Gambetta, F. Carollo, A. Lazarides, I. Lesanovsky, and J. P. Garrahan, Classical stochastic discrete time crystals, *Phys. Rev. E* **100**, 060105(R) (2019).
- [27] F. Iemini, A. Russomanno, J. Keeling, M. Schirò, M. Dalmonte, and R. Fazio, Boundary Time Crystals, *Phys. Rev. Lett.* **121**, 035301 (2018).
- [28] M. Medenjak, B. Buča, and D. Jaksch, The isolated Heisenberg magnet as a quantum time crystal, *Phys. Rev. B* **102**, 041117(R) (2020).
- [29] B. Buča, J. Tindall, and D. Jaksch, Non-stationary coherent quantum many-body dynamics through dissipation, *Nat. Commun.* **10**, 1730 (2019).
- [30] V. K. Kozin and O. Kyriienko, Quantum Time Crystals from Hamiltonians with Long-Range Interactions, *Phys. Rev. Lett.* **123**, 210602 (2019).
- [31] L. Bertini, A. De Sole, D. Gabrielli, G. Jona-Lasinio, and C. Landim, Current Fluctuations in Stochastic Lattice Gases, *Phys. Rev. Lett.* **94**, 030601 (2005).
- [32] T. Bodineau and B. Derrida, Distribution of current in nonequilibrium diffusive systems and phase transitions, *Phys. Rev. E* **72**, 066110 (2005).
- [33] R. J. Harris, A. Rakos, and G. M. Schutz, Current fluctuations in the zero-range process with open boundaries, *J. Stat. Mech.* (2005) P08003.
- [34] L. Bertini, A. De Sole, D. Gabrielli, G. Jona-Lasinio, and C. Landim, Nonequilibrium current fluctuations in stochastic lattice gases, *J. Stat. Phys.* **123**, 237 (2006).
- [35] T. Bodineau and B. Derrida, Cumulants and large deviations of the current through non-equilibrium steady states, *C. R. Phys.* **8**, 540 (2007).
- [36] V. Lecomte, C. Appert-Rolland, and F. van Wijland, Thermodynamic formalism for systems with Markov dynamics, *J. Stat. Phys.* **127**, 51 (2007).
- [37] J. P. Garrahan, R. L. Jack, V. Lecomte, E. Pitard, K. van Duijvendijk, and F. van Wijland, Dynamical First-Order Phase Transition in Kinetically Constrained Models of Glasses, *Phys. Rev. Lett.* **98**, 195702 (2007).
- [38] J. P. Garrahan, R. L. Jack, V. Lecomte, E. Pitard, K. van Duijvendijk, and F. van Wijland, First-order dynamical phase transition in models of glasses: an approach based on ensembles of histories, *J. Phys. A* **42**, 075007 (2009).
- [39] P. I. Hurtado and P. L. Garrido, Spontaneous Symmetry Breaking at the Fluctuating Level, *Phys. Rev. Lett.* **107**, 180601 (2011).
- [40] C. Ates, B. Olmos, J. P. Garrahan, and I. Lesanovsky, Dynamical phases and intermittency of the dissipative quantum Ising model, *Phys. Rev. A* **85**, 043620 (2012).
- [41] C. P. Espigares, P. L. Garrido, and P. I. Hurtado, Dynamical phase transition for current statistics in a simple driven diffusive system, *Phys. Rev. E* **87**, 032115 (2013).
- [42] R. J. Harris, V. Popkov, and G. M. Schütz, Dynamics of instantaneous condensation in the ZRP conditioned on an atypical current, *Entropy* **15**, 5065 (2013).
- [43] S. Vaikuntanathan, T. R. Gingrich, and P. L. Geissler, Dynamic phase transitions in simple driven kinetic networks, *Phys. Rev. E* **89**, 062108 (2014).
- [44] A. S. J. S. Mey, P. L. Geissler, and J. P. Garrahan, Rare-event trajectory ensemble analysis reveals metastable dynamical phases in lattice proteins, *Phys. Rev. E* **89**, 032109 (2014).
- [45] R. L. Jack, I. R. Thompson, and P. Sollich, Hyperuniformity and Phase Separation in Biased Ensembles of Trajectories for Diffusive Systems, *Phys. Rev. Lett.* **114**, 060601 (2015).
- [46] Y. Baek and Y. Kafri, Singularities in large deviation functions, *J. Stat. Mech.* **2015**, P08026 (2015).
- [47] O. T. Nyawo and H. Touchette, A minimal model of dynamical phase transition, *Europhys. Lett.* **116**, 50009 (2016).
- [48] R. J. Harris and H. Touchette, Phase transitions in large deviations of reset processes, *J. Phys. A* **50**, 10LT01 (2017).
- [49] A. Lazarescu, Generic dynamical phase transition in one-dimensional bulk-driven lattice gases with exclusion, *J. Phys. A* **50**, 254004 (2017).
- [50] K. Brandner, V. F. Maisi, J. P. Pekola, J. P. Garrahan, and C. Flindt, Experimental Determination of Dynamical Lee-Yang Zeros, *Phys. Rev. Lett.* **118**, 180601 (2017).
- [51] D. Karevski and G. M. Schütz, Conformal Invariance in Driven Diffusive Systems at High Currents, *Phys. Rev. Lett.* **118**, 030601 (2017).
- [52] F. Carollo, J. P. Garrahan, I. Lesanovsky, and C. Pérez-Espigares, Fluctuating hydrodynamics, current fluctuations, and hyperuniformity in boundary-driven open quantum chains, *Phys. Rev. E* **96**, 052118 (2017).
- [53] Y. Baek, Y. Kafri, and V. Lecomte, Dynamical Symmetry Breaking and Phase Transitions in Driven Diffusive Systems, *Phys. Rev. Lett.* **118**, 030604 (2017).
- [54] N. Tizón-Escamilla, C. Pérez-Espigares, P. L. Garrido, and P. I. Hurtado, Order and Symmetry-Breaking in the Fluctuations of Driven Systems, *Phys. Rev. Lett.* **119**, 090602 (2017).

- [55] O. Shpielberg, Geometrical interpretation of dynamical phase transitions in boundary-driven systems, *Phys. Rev. E* **96**, 062108 (2017).
- [56] Y. Baek, Y. Kafri, and V. Lecomte, Dynamical phase transitions in the current distribution of driven diffusive channels, *J. Phys. A* **51**, 105001 (2018).
- [57] O. Shpielberg, T. Nemoto, and J. Caetano, Universality in dynamical phase transitions of diffusive systems, *Phys. Rev. E* **98**, 052116 (2018).
- [58] C. Pérez-Espigares, I. Lesanovsky, J. P. Garrahan, and R. Gutiérrez, Glassy dynamics due to a trajectory phase transition in dissipative Rydberg gases, *Phys. Rev. A* **98**, 021804(R) (2018).
- [59] P. Chleboun, S. Grosskinsky, and A. Pizzoferrato, Current large deviations for partially asymmetric particle systems on a ring, *J. Phys. A* **51**, 405001 (2018).
- [60] K. Klymko, P. L. Geissler, J. P. Garrahan, and S. Whitelam, Rare behavior of growth processes via umbrella sampling of trajectories, *Phys. Rev. E* **97**, 032123 (2018).
- [61] S. Whitelam, Large deviations in the presence of cooperativity and slow dynamics, *Phys. Rev. E* **97**, 062109 (2018).
- [62] H. Vroylandt and G. Verley, Non-equivalence of dynamical ensembles and emergent non-ergodicity, *J. Stat. Phys.* **174**, 404 (2019).
- [63] H. Touchette, The large deviation approach to statistical mechanics, *Phys. Rep.* **478**, 1 (2009).
- [64] B. Derrida, Non-equilibrium steady states: Fluctuations and large deviations of the density and of the current, *J. Stat. Mech.* (2007) P07023.
- [65] P. I. Hurtado, C. P. Espigares, J. J. del Pozo, and P. L. Garrido, Thermodynamics of currents in nonequilibrium diffusive systems: Theory and simulation, *J. Stat. Phys.* **154**, 214 (2014).
- [66] A. Lazarescu, The physicist's companion to current fluctuations: One-dimensional bulk-driven lattice gases, *J. Phys. A* **48**, 503001 (2015).
- [67] C. Pérez-Espigares and P. I. Hurtado, Sampling rare events across dynamical phase transitions, *Chaos* **29**, 083106 (2019).
- [68] F. Carollo, J. P. Garrahan, and I. Lesanovsky, Current fluctuations in boundary-driven quantum spin chains, *Phys. Rev. B* **98**, 094301 (2018).
- [69] F. Spitzer, Interaction of Markov processes, *Adv. Math.* **5**, 246 (1970).
- [70] B. Derrida, An exactly soluble non-equilibrium system: The asymmetric simple exclusion process, *Phys. Rep.* **301**, 65 (1998).
- [71] B. Derrida and J. L. Lebowitz, Exact Large Deviation Function in the Asymmetric Exclusion Process, *Phys. Rev. Lett.* **80**, 209 (1998).
- [72] O. Golinelli and K. Mallick, The asymmetric simple exclusion process: An integrable model for non-equilibrium statistical mechanics, *J. Phys. A* **39**, 12679 (2006).
- [73] J. L. Doob, Conditional Brownian motion and the boundary limits of harmonic functions, *Bull. Soc. Math. Fr.* **85**, 431 (1951).
- [74] R. Chetrite and H. Touchette, Variational and optimal control representations of conditioned and driven processes, *J. Stat. Mech.* (2015) P12001.
- [75] R. Chetrite and H. Touchette, Nonequilibrium Markov processes conditioned on large deviations, *Ann. Inst. Henri Poincaré* **16**, 2005 (2015).
- [76] L. Bertini, A. De Sole, D. Gabrielli, G. Jona-Lasinio, and C. Landim, Macroscopic fluctuation theory, *Rev. Mod. Phys.* **87**, 593 (2015).
- [77] F. Carollo, J. P. Garrahan, I. Lesanovsky, and C. Pérez-Espigares, Making rare events typical in Markovian open quantum systems, *Phys. Rev. A* **98**, 010103(R) (2018).
- [78] D. Simon, Construction of a coordinate Bethe ansatz for the asymmetric simple exclusion process with open boundaries, *J. Stat. Mech.* (2009) P07017.
- [79] R. L. Jack and P. Sollich, Large deviations and ensembles of trajectories in stochastic models, *Prog. Theor. Phys. Suppl.* **184**, 304 (2010).
- [80] V. Popkov, G. M. Schütz, and D. Simon, ASEP on a ring conditioned on enhanced flux, *J. Stat. Mech.* (2010) P10007.
- [81] Y. Kuramoto, *Chemical Oscillations, Waves and Turbulence* (Springer, New York, 1984).
- [82] Y. Kuramoto and I. Nishikawa, Statistical macrodynamics of large dynamical systems. Case of a phase transition in oscillator communities, *J. Stat. Phys.* **49**, 569 (1987).
- [83] A. Pikovsky, M. Rosenblum, and J. Kurths, *Synchronization: A Universal Concept in Nonlinear Sciences* (Cambridge University Press, Cambridge, 2003).
- [84] J. A. Acebrón, L. L. Bonilla, C. J. Pérez Vicente, F. Ritort, and R. Spigler, The Kuramoto model: A simple paradigm for synchronization phenomena, *Rev. Mod. Phys.* **77**, 137 (2005).
- [85] A. De Masi, E. Presutti, and E. Scacciatelli, The weakly asymmetric simple exclusion process, *Ann. Inst. Henri Poincaré* **25**, 1 (1989), http://www.numdam.org/item/AIHPB_1989_25_1_1_0/.
- [86] J. Gärtner, Convergence towards Burger's equation and propagation of chaos for weakly asymmetric exclusion processes, *Stoch. Proc. Appl.* **27**, 233 (1987).
- [87] G. M. Schutz, Exactly solvable models for many-body systems far from equilibrium, *Phase Transitions Crit. Phenom.* **19**, 1 (2001).
- [88] H. Spohn, *Large Scale Dynamics of Interacting Particles*, Theoretical and Mathematical Physics (Springer Berlin Heidelberg, Berlin, Heidelberg, 2012).
- [89] J. P. Garrahan, Aspects of non-equilibrium in classical and quantum systems: Slow relaxation and glasses, dynamical large deviations, quantum non-ergodicity, and open quantum dynamics, *Physica (Amsterdam)* **504A**, 130 (2018).
- [90] S. Kaviani and F. H. Jafarpour, Current fluctuations in a stochastic system of classical particles with next-nearest-neighbor interactions, *J. Stat. Mech.* (2020) 013210.
- [91] A. Prados, A. Lasanta, and P. I. Hurtado, Nonlinear driven diffusive systems with dissipation: Fluctuating hydrodynamics, *Phys. Rev. E* **86**, 031134 (2012).
- [92] P. I. Hurtado, A. Lasanta, and A. Prados, Typical and rare fluctuations in nonlinear driven diffusive systems with dissipation, *Phys. Rev. E* **88**, 022110 (2013).
- [93] A. Lasanta, A. Manacorda, A. Prados, and A. Puglisi, Fluctuating hydrodynamics and mesoscopic effects of spatial correlations in dissipative systems with conserved momentum, *New J. Phys.* **17**, 083039 (2015).

- [94] A. Lasanta, P. I. Hurtado, and A. Prados, Statistics of the dissipated energy in driven diffusive systems, *Eur. Phys. J. E* **39**, 35 (2016).
- [95] A. Manacorda, C. A. Plata, A. Lasanta, A. Puglisi, and A. Prados, Lattice models for granular-like velocity fields: Hydrodynamic description, *J. Stat. Phys.* **164**, 810 (2016).
- [96] C. Gutiérrez-Ariza and P. I. Hurtado, The kinetic exclusion process: A tale of two fields, *J. Stat. Mech.* (2019) 103203.
- [97] Q. H. Wei, C. Bechinger, and P. Leiderer, Single-file diffusion of colloids in one-dimensional channels, *Science* **287**, 625 (2000).
- [98] C. Lutz, M. Kollmann, and C. Bechinger, Single-File Diffusion of Colloids in One-Dimensional Channels, *Phys. Rev. Lett.* **93**, 026001 (2004).
- [99] K. Ladavac and D. G. Grier, Colloidal hydrodynamic coupling in concentric optical vortices, *Europhys. Lett.* **70**, 548 (2005).
- [100] Y. Roichman, D. G. Grier, and G. Zaslavsky, Anomalous collective dynamics in optically driven colloidal rings, *Phys. Rev. E* **75**, 020401(R) (2007).
- [101] Y. Roichman and D. G. Grier, Three-dimensional holographic ring traps, in *Complex Light and Optical Forces*, edited by D. L. Andrews, E. J. Gálvez, and G. Nienhuis (International Society for Optics and Photonics (SPIE), Bellingham, 2007), Vol. 6483, p. 131.
- [102] A. Kumar and J. Bechhoefer, Optical feedback tweezers, in *Optical Trapping and Optical Micromanipulation XV* edited by K. Dholakia and G. C. Spalding (International Society for Optics and Photonics (SPIE), Bellingham, 2018), Vol. 10723, p. 282.
- [103] D. G. Grier, Optical tweezers in colloid and interface science, *Curr. Opin. Colloid Interface Sci.* **2**, 264 (1997).
- [104] A. Ortiz-Ambriz, J. C. Gutiérrez-Vega, and D. Petrov, Manipulation of dielectric particles with nondiffracting parabolic beams, *J. Opt. Soc. Am. A* **31**, 2759 (2014).
- [105] I. A. Martínez, E. Roldán, L. Dinis, Dmitri Petrov, and R. A. Rica, Adiabatic Processes Realized with a Trapped Brownian Particle, *Phys. Rev. Lett.* **114**, 120601 (2015).
- [106] I. A. Martínez, E. Roldán, L. Dinis, and R. A. Rica, Colloidal heat engines: A review, *Soft Matter* **13**, 22 (2017).
- [107] J. A. Rodrigo, M. Angulo, and T. Alieva, Dynamic morphing of 3d curved laser traps for all-optical manipulation of particles, *Opt. Express* **26**, 18608 (2018).
- [108] N. Tizón-Escamilla, P. I. Hurtado, and P. L. Garrido, Structure of the optimal path to a fluctuation, *Phys. Rev. E* **95**, 032119 (2017).